Journal of Magnetic Resonance 206 (2010) 241–245

Contents lists available at ScienceDirect

Journal of Magnetic Resonance

journal homepage: www.elsevier.com/locate/jmr

^{1}H Homonuclear dipolar decoupling using symmetry-based pulse sequences at ultra fast magic-angle spinning frequencies

Subhradip Paul [a], Denis Schneider [b], P.K. Madhu [a,*]

[a] Department of Chemical Sciences, Tata Institute of Fundamental Research, Homi Bhabha Road, Colaba, Mumbai 400 005, India
[b] Solids NMR Applications, Bruker Biospin GmbH, Silberstreifen 4, 76287 Rheinstetten, Germany

ARTICLE INFO

Article history:
Received 2 June 2010
Revised 18 July 2010
Available online 27 July 2010

Keywords:
Solid-state NMR
Homonuclear dipolar decoupling
Ultrafast MAS
RN_n^ν
*w*PMLG

ABSTRACT

We demonstrate here the application of symmetry-based pulse sequences for homonuclear dipolar decoupling in solid-state NMR at magic-angle spinning (MAS) frequencies up to 65 kHz using moderate radiofrequency (RF) amplitudes. Theoretical arguments favouring the requirement of low RF amplitudes at high MAS frequencies are given for these sequences. A comparison with *w*PMLG$_{mm}^{x\bar{x}}$ is given at 65 kHz of MAS frequency to emphasise that the symmetry-based pulse sequences have a lower RF amplitude requirement at high MAS frequencies.

1. Introduction

^{1}H solid-state nuclear magnetic resonance (NMR) spectra are plagued by poor resolution due to the presence of strong homonuclear dipole–dipole couplings between the abundant ^{1}H spins. This often obscures the chemical-shift information. The only way to obtain high-resolution spectra of ^{1}H is to apply radiofrequency (RF) pulses in combination with magic-angle spinning (MAS), popularly known as combined rotation and multiple-pulse spectroscopy (CRAMPS) [1–3]. Several CRAMPS techniques have been developed over the years, significant ones under MAS being phase modulated Lee-Goldburg (PMLG) [4–6], decoupling using mind boggling optimisation (DUMBO) [7,8], symmetry-based sequences like RN_n^ν [9–11], and smooth amplitude modulation (SAM) [12,13]. With the advent of probes capable of yielding up to 65 kHz of MAS frequency, the main focus of decoupling is shifted towards development of pulse schemes which can be applied at such high MAS frequencies.

Introduction of supercycled schemes for PMLG has enabled its application at moderate to high MAS frequencies up to 65 kHz [14,15] and has been substantiated theoretically [16]. Subsequently DUMBO and SAM have been applied at high MAS frequencies [13,16,17]. One major disadvantage of *w*PMLG and *w*DUMBO sequences is the requirement of high RF amplitudes (ν_1) at higher MAS frequencies which restricts the application of these sequences to low or moderate MAS frequencies [15]. At certain ratios of MAS frequencies (ν_r) and cycle frequency (ν_c) of the RF sequence resonant interference occurs and is manifested by the presence of extra lines in the spectrum [18]. When these lines fall on the spectrum they lead to line broadening and avoiding such resonance condition requires prior theoretical understanding and careful experimental optimisation. A different approach is the use of symmetry-based pulse sequences developed by Demco et al., and the group of Levitt [9,19,20]. There are two different classes of sequences which have been developed using the principle of symmetry of spin interactions. One uses composite 180° pulses whilst the other utilises smooth amplitude modulation [9–13]. A review of the sequences which have been already implemented at moderate to high MAS frequencies up to 65 kHz is given in Refs. [21–23].

We have demonstrated the application of RN_n^ν sequences at moderate MAS frequencies [10,11]. In the present work we demonstrate the application of RN_n^ν sequences up to a spinning frequency of 65 kHz. A theoretical description will be given indicating that with the increase of ν_r, the required ν_1 for efficient decoupling is not as high as the other sequences and this will be corroborated by experimental findings. A comparison between RN_n^ν and *w*PMLG$_{mm}^{x\bar{x}}$ will be given at the MAS frequency of 65 kHz to show that similar resolution can be obtained using the former at a lower RF amplitude.

2. Theory

The RN_n^ν symmetry sequences used here are of the form $\left[R_\phi R'_{-\phi}\right]^{N/2}$ and consist of $\frac{N}{2}$ pairs of the pulse block $\left[R_\phi R'_{-\phi}\right]$

* Corresponding author. Fax: +91 22 2280 4610.
E-mail address: madhu@tifr.res.in (P.K. Madhu).

1090-7807/$ - see front matter © 2010 Elsevier Inc. All rights reserved.
doi:10.1016/j.jmr.2010.07.013

spanning n rotor periods, where ϕ is the overall phase shift given by $\phi = \frac{\pi}{N}\nu$. The element R_ϕ is derived from the basic element R^0 by an overall phase shift of ϕ. The element $R'_{-\phi}$ is derived from R_ϕ by changing the sign of all phases. The basic element R^0 rotates resonant spins by an odd multiple of π about the x-axis. Typically, the basic element R^0 is a single or composite 180° pulse [24]. For better performance with respect to off-resonance and in order to improve local averaging of the homonuclear dipolar interactions, the RN_n^ν sequences used here are based on the composite pulse elements [9–11]. Here, the element is $R^0 = 90_{-45}90_{45}90_{-45}$. The RN_n^ν sequences suitable for homonuclear dipolar decoupling are such that $\frac{\nu}{N} = \frac{1}{2}$. The RN_n^ν sequences used here are explicitly given by

$$RN_n^\nu = \{(90_{-45}90_{45}90_{-45})_{90}(90_{45}90_{-45}90_{45})_{-90}\}^{N/2} \quad (1)$$

$$= \{(90_{45}90_{135}90_{45})(90_{-45}90_{-135}90_{-45})\}^{N/2} \quad (2)$$

A table of RN_n^ν sequences suitable for homonuclear decoupling is given in Table 1.

The symmetry-based sequences are analysed here by treating a system of coupled proton spins using bimodal Floquet theory [25,26]. In case of the symmetry sequences discussed here, the cycle frequency (ν_c) of the pulse sequence and the MAS frequency (ν_r) can be related to each other by $\nu_c = \frac{N}{2n}\nu_r$. Hence, the symmetry sequences in principle can be theoretically treated utilising average Hamiltonian theory or single-mode Floquet theory as has been done earlier [18,24]. Here we chose to treat the sequences using bimodal Floquet theory in order to investigate the scenario where possible deviations from the rotor-synchronisation come in and the two characteristic frequencies ν_c and ν_r become incommensurate. Such a case will be presented in detail later.

The Floquet Hamiltonian in the RF interaction frame can be represented as [18]:

$$\mathscr{H} = \sum_{n,k}\left(\mathscr{H}_{0k}^{CS} + \mathscr{H}_{nk}^{DD}\right) + \nu_c N^c + \nu_r N^r \quad (3)$$

where $\mathscr{H}^{CS}$ and $\mathscr{H}^{DD}$ correspond to the isotropic chemical-shift and homonuclear dipolar Hamiltonian given by

$$\mathscr{H}_{0k}^{CS} = \sum_{m,a}\Delta\nu_a d_{m,k}^{(1)} T_{m,a}^{(1)} F_0^r F_k^c \quad (4)$$

$$\mathscr{H}_{nk}^{DD} = \sum_{m,a<b}\nu_{ab} G_{ab}^n d_{m,k}^{(2)} T_{m,ab}^{(2)} F_n^r F_k^c \quad (5)$$

Here, the interactions included are the isotropic chemical-shift of the a spins, $\Delta\nu_a$, and the homonuclear dipolar interaction between the spins a and b, the strength of which is given by ν_{ab}. The CSA of the proton spins is neglected owing to its relatively small magnitude. The spin parts of the interactions are characterised by the irreducible tensor operators $T_m^{(l)}$. The geometric spatial dependence of the anisotropic dipolar Hamiltonian is characterised by the G^n coefficients [26]. N and F are the number and ladder operators, respectively [27]. $d_{m,k}^{(l)}$ are the Fourier coefficients, the magnitude of which is dependent on the RF pulse sequence. A complete representation of these operators and coefficients is given in Ref. [18].The efficiency of decoupling due to a sequence is dependent on these coefficients whose magnitude is determined by the RF amplitude ν_1 and the cycle frequency of the sequence ν_c which includes the length of the window (w), in case of a windowed sequence. In case of the RN_n^ν sequence used here, the cycle time is given by the total duration of the pulse block $\left[R_\phi R'_{-\phi}\right]$ which is equivalent to a 540° pulse. For the convenience of the reader, it is noteworthy to mention that n in Eq. (3) denotes the order of the Hamiltonian whilst n in RN_n^ν sequence represents the number of rotor periods the RN_n^ν sequences span, i.e. the space winding number.

Table 1
RN_n^ν symmetries for the observation of isotropic chemical-shifts and heteronuclear J couplings under MAS. All the mentioned RN_n^ν sequences select isotropic chemical-shift terms suppressing the CSA and homonuclear DD coupling terms. All inequivalent symmetries in the range of $N \leqslant 20$, $n \leqslant 5$ and $\nu \leqslant 10$ are shown.

$n = 1$	$R6_1^3$ $R8_1^4$ $R10_1^5$ $R12_1^6$ $R14_1^7$ $R16_1^8$ $R18_1^9$ $R20_1^{10}$
$n = 2$	$R6_2^3$ $R10_2^5$ $R14_2^7$ $R18_2^9$
$n = 3$	$R8_3^4$ $R10_3^5$ $R14_3^7$ $R16_3^8$ $R20_3^{10}$
$n = 4$	$R6_4^3$ $R10_4^5$ $R14_4^7$ $R18_4^9$
$n = 5$	$R6_5^3$ $R8_5^4$ $R12_5^6$ $R14_5^7$ $R16_5^8$ $R18_5^9$

To compare the efficiency of decoupling, it is required to derive an effective Hamiltonian. The derivation of the effective Hamiltonian requires application of van Vleck transformation to the Hamiltonian given in Eq. (3) [28]. Truncating the small and non-significant terms, the Hamiltonian derived after the van Vleck transformation is given by

$$\widetilde{\mathscr{H}} = \widetilde{\mathscr{H}}_{00}^{CS(0)} + \sum_{n,k}\widetilde{\mathscr{H}}_{nk}^{DD(1)} + \nu_r N^r + \nu_c N^c \quad (6)$$

where

$$\widetilde{\mathscr{H}}_{00}^{CS(0)} = \sum_{m,a}\Delta\nu_a d_{m,0}^{(1)} T_{m,a}^{(1)} F_0^r F_0^c \quad (7)$$

$$\widetilde{\mathscr{H}}_{nk}^{DD(1)} = -\frac{1}{2}\sum_{n',a<b,b<c}\nu_{ab}\nu_{bc} G_{ab}^{n'} G_{bc}^{n-n'} \sum_{k,m,m'}\Delta_{mm'}^{n'k}\left[T_{m,ab}^{(2)}, T_{m',bc}^{(2)}\right] F_n^r F_k^c \quad (8)$$

with

$$\Delta_{mm'}^{n'k} = \frac{d_{m,k'}^{(2)} d_{m',k-k'}^{(2)}}{n'\nu_r + k'\nu_c} \quad (9)$$

Following Haeberlen's notation [29] for numbering various orders of Hamiltonian, $\widetilde{\mathscr{H}}_{00}^{CS(0)}$ is the zero-order (diagonal) chemical-shift contribution whilst $\widetilde{\mathscr{H}}_{nk}^{DD(1)}$ is the first-order (diagonal and off-diagonal) dipolar coupling contribution to the interaction Hamiltonian. The diagonal blocks of this Hamiltonian can be written as:

$$\widetilde{\mathscr{H}} = \left(\widetilde{\mathscr{H}}_{00}^{CS(0)} + \widetilde{\mathscr{H}}_{00}^{DD(1)}\right) + \nu_r N^r + \nu_c N^c \quad (10)$$

which is obtained by substituting $n = k = 0$ in Eq. (6). As long as the non-significant off-diagonal block elements of the Hamiltonian given by Eq. (6) are ignored, the Hamiltonian given by Eq. (10) can be used to determine the decoupling efficiency of a particular decoupling sequence. The $\Delta_{mm'}^{n'k}$ coefficients for the block diagonal Hamiltonian can be written as

$$\Delta_{mm'}^{n'0} = \frac{d_{m,k'}^{(2)} d_{m',-k'}^{(2)}}{n'\nu_r + k'\nu_c} \quad (11)$$

For convenience of notation we change the indices n' by n and k' by k and thus the Δ – coefficients can be defined as

$$\Delta_{mm'}^{nk} = \frac{d_{m,k}^{(2)} d_{m',-k}^{(2)}}{n\nu_r + k\nu_c} \quad (12)$$

Decoupling implies reduction in the magnitude of the dipolar contribution by the application of MAS and RF simultaneously. The magnitude of $\Delta_{mm'}^{nk}$ in Eq. (12) reflects the amount of decoupling that can be achieved by a particular RF sequence. However, when $n\nu_r + k\nu_c = 0$, the off-diagonal blocks in the Floquet Hamiltonian become significant and $< n'k' \left| \widetilde{\mathscr{H}}_{nk}^{DD(1)} \right| n''k'' > \neq 0$, with $|n| = |n' - n''| =$ 1–4 and $|k| = |k' - k''| \neq 0$. Thus two major degeneracy conditions arise which must be avoided:

(a) $kv_c = v_r$ *or* $2v_r$: This synchronisation leads to degeneracies between the elements with $n = 1, 2$ and $|k| = 1,2,3,4,\ldots$. In this case the zero-order off-diagonal elements become significantly large and van Vleck transformation cannot be performed and direct diagonalisation is the only way [18,30]. This condition is known as the zero-order degeneracy condition and it leads to severe line broadening.

(b) $kv_c = 3v_r$ *or* $4v_r$: In this case van Vleck transformation can be done, but the diagonal blocks of $n = 3, 4$ and $|k| = 1,2,3,4,\ldots$ are connected by elements formed by the first-order van Vleck transformation. This condition is known as the first-order degeneracy condition and their effect is less pronounced. If these resonance conditions fall on the spectra, they lead to line broadening [18,30].

Higher-order degeneracies are possible but their contribution is not significantly large and can be ignored in the present context. For convenience a parameter ψ can be defined as $\psi = \frac{v_c}{v_r}$ and it can be stated that $\psi = \frac{1}{k}, \frac{2}{k}, \frac{3}{k}, \frac{4}{k}$ must be avoided to obtain efficient decoupling, where k can have all possible integer values. The actual amount of line narrowing depends on the magnitude of the dipolar Hamiltonian which involves further multiplication of complex factors to the $\Delta^{nk}_{mm'}$ coefficients given in Eq. (12). So the value of the $\Delta^{nk}_{mm'}$-coefficients only gives a rough estimate of the amount of decoupling that can be achieved by a particular RF pulse scheme. Each decoupling scheme has its own distribution of $d^{(2)}_{m,k}$ Fourier coefficients and the presence of MAS frequency in the denominator of Eq. (12) creates a shift in the averaging over the Fourier coefficients.

In order to gain an insight into the averaging effect of MAS over the Fourier coefficients, we calculate here sum of the $\Delta^{nk}_{mm'}$-coefficients over all the four indices (n, k, m, m') with n index running up to $n = 2$, as given in Eq. (12), for the RN^{ν}_{n} sequences given in Table 1 that require $\nu_1 < 300$ kHz at $\nu_r = 35$, 45, 55, and 65 kHz. The results are shown in Fig. 1. The arrows on the curve indicate the RN^{ν}_{n} sequences chosen for the experimental purpose. The salient features of the curves are as follows:

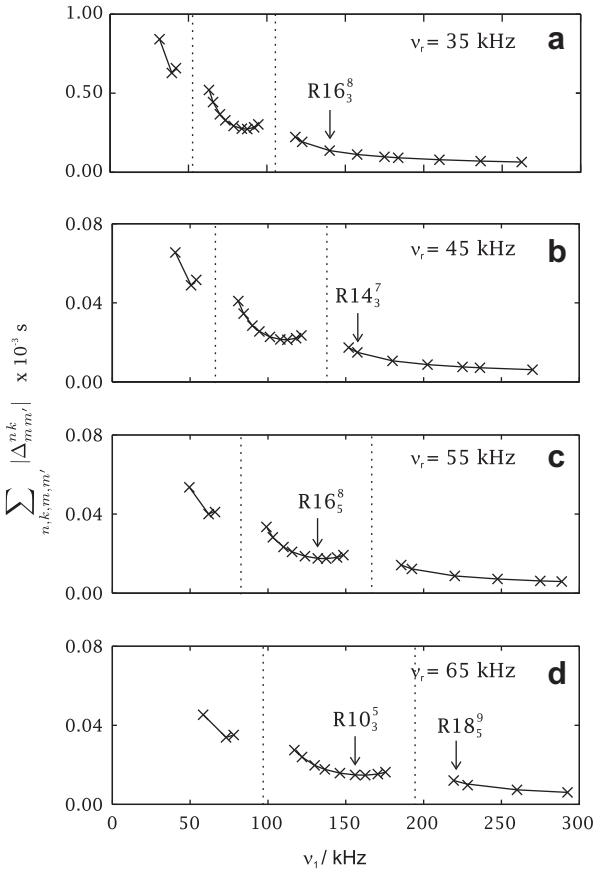

Fig. 1. Sum over all the four indices for the $\Delta^{nk}_{mm'}$-coefficient given in Eq. (12) calculated for all the RN^{ν}_{n} sequences given in Table 1 sequences which have RF requirement $\nu_1 \leqslant 300$ kHz. The calculations were done at four different MAS frequencies: (a) 35 kHz, (b) 45 kHz, (c) 55 kHz, and (d) 65 kHz. The RN^{ν}_{n} sequences used in the experiments at the respective spinning frequencies are indicated on the figure. The vertical dotted lines show $\psi = 1$ (left) and $\psi = 2$ (right) conditions respectively.

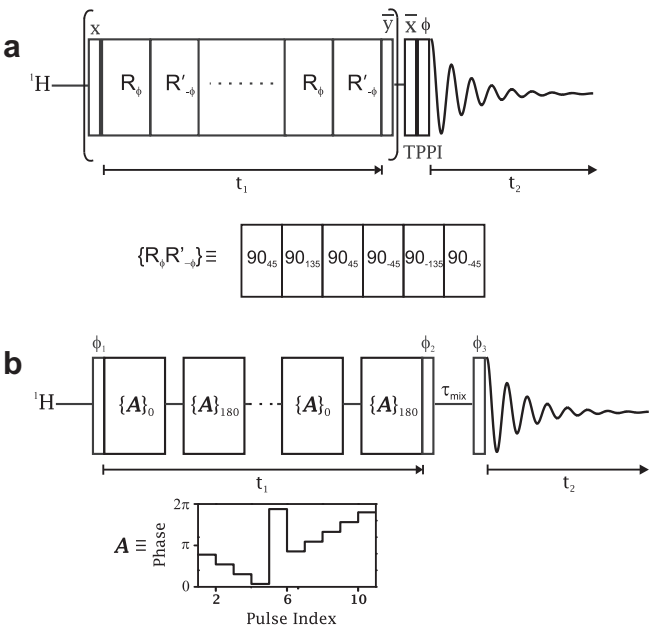

Fig. 2. (a) Schematics of the pulse sequence utilising RN^{ν}_{n} sequences to obtain high-resolution spectra of ^{1}H. The phases of the 90° pulses are indicated on top of the pulses. The phase ϕ on the final pulse indicates a phase cycling of $[x, y, \bar{x}, \bar{y}]$ which is followed by the receiver. Schematic of the RN^{ν}_{n} block is given below the pulse sequence. (b) Schematic of the pulse sequence utilising wPMLG$^{xx}_{mm}$ for homonuclear dipolar decoupling in the indirect dimension. The supercycling of the PMLG block is indicated on the figure. ***A*** depicts the phase profile of a w PMLG block. The 90° pulses are phase cycled as $\phi_1 = [x, y, \bar{x}, \bar{y}]$, $\phi_2 = [\bar{x}, \bar{y}, x, y]$, and $\phi_3 = [x, y, \bar{x}, \bar{y}]$. The receiver follows the phases of the last pulse 90° pulse.

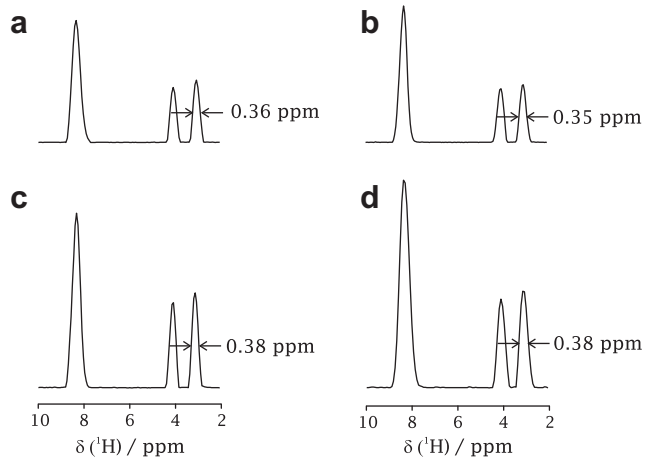

Fig. 3. Skyline projections of the indirect dimension of 2D correlation spectra of glycine obtained with the pulse sequence shown in Fig. 2a. The spectra were acquired with (a) $R16^8_3$ at $\nu_r = 35$ kHz, (b) $R14^7_3$ at $\nu_r = 45$ kHz, (c) $R16^8_5$ at $\nu_r = 55$ kHz, and (d) $R10^5_3$ at $\nu_r = 65$ kHz. The experimental details are indicated in the text. The spectra were scaled up by a factor of 0.6.

- The curves show discontinuity around $\psi = 1, 2$ as these are the recoupling conditions for homonuclear dipolar couplings.
- As we go to higher MAS frequencies, the overall magnitude of the $\sum_{n,k,m,m'} \Delta^{nk}_{mm'}$ becomes lower in the region $\psi < 2$.
- For any given ν_r the magnitude of $\sum_{n,k,m,m'} \Delta^{nk}_{mm'}$ decreases with increase in ν_1 and subsequently ν_c as ν_c is related to ν_1 by $\nu_c = \frac{2}{3}\nu_1$ in case of the RN^{ν}_{n} sequences.
- In the spinning frequency regime $\nu_r \leqslant 45$ kHz it is advisable to work in the region $\psi > 2$, whilst at $\nu_r > 45$ kHz, it is possible to work in the $1 < \psi < 2$ region. This can then lead to the implementation of RN^{ν}_{n} sequences at lower RF amplitudes at higher MAS frequencies, a feature not quite shared by the other homonuclear dipolar decoupling schemes.

Similar calculations have been done earlier for wPMLG$^{x\bar{x}}_{mm}$ for high MAS frequencies [15] and have been experimentally verified by Mao and Pruski for spinning frequencies $\nu_r > 10$ kHz [31].

3. Experimental

The experiments were carried out on a Bruker AVIII 600 MHz wide-bore spectrometer using a 1.3 mm triple resonance (HCN) probe. Commercially available glycine and L-histidine·HCl·H_2O were used without further purification or crystallisation. A sample of commercially available adamantane was used for the proton RF calibration via nutation experiments.

4. Results and discussion

In order to obtain high-resolution spectra of ^{1}H the RN^{ν}_{n} sequences were applied in a two-dimensional (2D) fashion as shown in Fig. 2a. The details of the design of this pulse sequence were given in an earlier work [11]. Homonuclear decoupling is achieved in the indirect domain where the magnetisation evolves under the decoupling sequence whilst only MAS is performed in the direct dimension. A projection along the indirect dimension gives the high-resolution ^{1}H spectra.

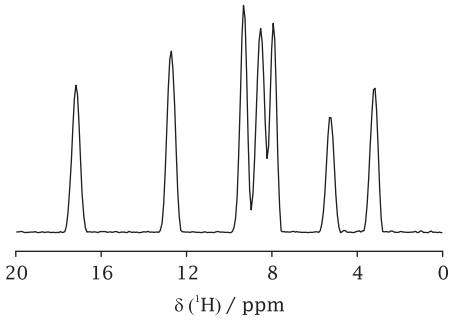

Fig. 4. Skyline projection of the indirect dimension of 2D correlation spectrum of L-histidine·HCl·H_2O obtained with the pulse sequence shown in Fig. 2a. The spectrum was acquired with $R10^5_3$ at $\nu_r = 65$ kHz and was scaled up by a factor of 0.6. The rest of the experimental details are included in the text.

Fig. 3 shows the spectra of glycine obtained at $\nu_r = 35$, 45, 55, and 65 kHz using (a) $R16^8_3$, (b) $R14^7_3$, (c) $R16^8_5$, and (d) $R10^5_3$. The RF amplitudes required are 140 kHz, 157.5 kHz, 132 kHz, and 162.5 kHz respectively. One-thousand and twenty-four points were taken in the indirect dimension with 4 s of recycle delay between each of the four scans. The spectra of glycine were referenced by assigning the midpoint of the two methylene proton resonances to be at 3.55 ppm. The scaling factor in all the cases was found to be 0.6. The carrier frequency on the ^{1}H was kept at -10 kHz from the centre of the ^{1}H spectra. The mentioned linewidths imply that going from lower to higher MAS frequency does not result in much increase in resolution but compared to other decoupling sequences like wPMLG$^{x\bar{x}}_{mm}$ or wDUMBO, there is a noticeable gain in RF amplitude [15].

Fig. 4 shows the spectrum of L-histidine·HCl·H_2O obtained at $\nu_r = 65$ kHz and $\nu_1 = 162.5$ kHz using $R10^8_3$. One-thousand and twenty-four points were taken in the indirect dimension with 4 s of recycle delay between each of the four scans. The spectrum of L-histidine·HCl·H_2O was referenced by assigning the methylene resonance to be at 3.2 ppm. The scale factor was found to be 0.6. The carrier frequency was kept at -10 kHz from the centre of the ^{1}H spectra.

Fig. 5 shows a comparison between wPMLG$^{x\bar{x}}_{mm}$ and RN^{ν}_{n} sequences at 65 kHz of MAS frequency. The 2D pulse sequence with wPMLG$^{x\bar{x}}_{mm}$ is shown in Fig. 2b. For the comparison study both wPMLG$^{x\bar{x}}_{mm}$ and RN^{ν}_{n} sequences were applied in a 2D fashion with homonuclear decoupling in the indirect dimension and acquisition under MAS in the direct dimension. In both the cases 1024 points were collected with 4 s of recycle delay between each of the four scans. Fig. 5a shows the ^{1}H spectra of glycine obtained at 65 kHz using $R10^3_5$ whilst Fig. 5b shows the spectra obtained using the pulse sequence shown in Fig. 2b. For the wPMLG$^{x\bar{x}}_{mm}$ experiment the optimisation was done by collecting a series of 1D spectra using windowed acquisition. The optimal cycle frequency was found to be 40.65 kHz which includes a window duration of 2.7 μs. The carrier frequency was kept at +4 kHz from the centre of the proton frequency. The scaling factor for the wPMLG$^{x\bar{x}}_{mm}$ sequence was found to be 0.48. These optimal values correspond to those reported earlier [15]. The RF amplitude requirement for (a) is 162.5 kHz and that for (b) is 214 kHz. The linewidth shown on the figure indicates that the same resolution can be obtained using lower RF amplitude for RN^{ν}_{n} sequences at high MAS frequencies. From the data it can be inferred that RN^{ν}_{n} sequences can perform at lower RF amplitudes than wPMLG$^{x\bar{x}}_{mm}$ as we go to higher spinning

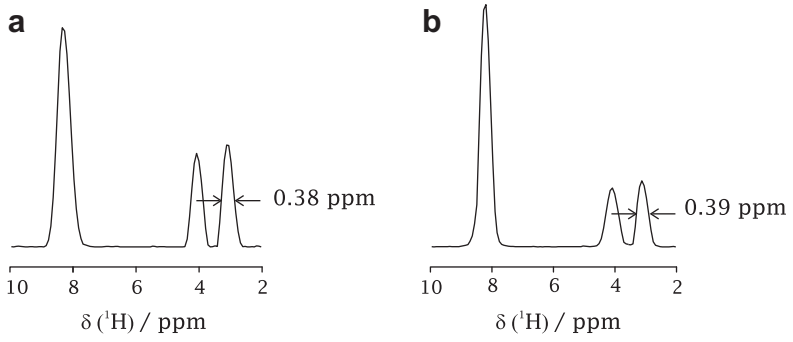

Fig. 5. Skyline projections of the indirect dimension of 2D correlation spectra of glycine spectra acquired with the pulse sequences shown in (a) Fig. 2a and (b) Fig. 2b. The experiments were performed at 65 kHz of MAS frequency. For the RN^{ν}_{n} sequence the spectrum was scaled up by a factor of 0.6 and for wPMLG$^{x\bar{x}}_{mm}$ by 0.48. The rest of the experimental details are discussed in the text.

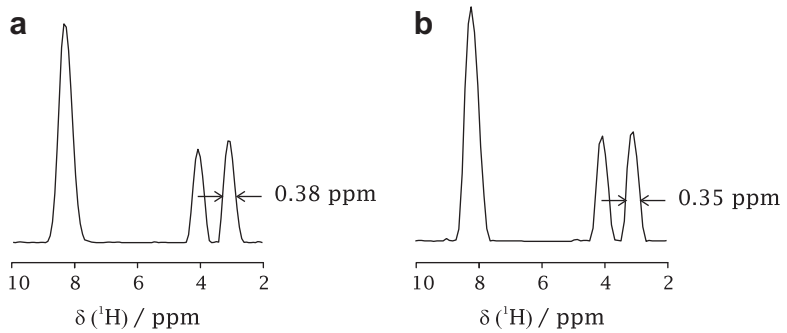

Fig. 6. Skyline projections of the indirect dimension of 2D correlation spectra of glycine acquired at $\nu_r = 65$ kHz using (a) $R10_3^5$ with $\nu_r = 162.5$ kHz and (b) $R18_5^9$ with $\nu_r = 219.4$ kHz. The spectra were scaled up by a factor of 0.6.

frequencies. In this context it can be also stated that RN_n^ν sequences with an effective x-axis of rotation is more suitable for 2D experiments where we achieve high resolution ^{1}H spectra in the indirect dimension whilst wPMLG$_{mm}^{xx}$ having an effective z-axis of rotation can be more conveniently applied in windowed fashion for 1D experiments.

Fig. 6 shows the spectra of glycine obtained at $\nu_r = 65$ kHz using (a) $R10_3^5$ and (b) $R18_4^9$ with RF amplitude of 162.5 kHz and 219.4 kHz respectively. The rest of the experimental parameters are the same as those in Fig. 3. The linewidth indicated on the figure shows that there is a slight gain in the resolution by 0.03 ppm at higher $\nu_1$which is also predicted by the theoretical calculation but the gain is not substantial as the $\Delta_{mm'}^{nk}$-coefficients have comparable magnitude below and above the $\psi = 2$ condition at high MAS frequencies. This observation validates our point that at high spinning frequencies it is possible and preferable to work below the $\psi = 2$ condition using lower RF amplitude. The theoretical calculation predicts that as we go to higher ψ values in the $\psi > 2$ region, we can achieve slightly better resolution but at the expense of higher RF amplitudes.

5. Conclusions

The potential of the symmetry-based RN_n^ν sequences towards homonuclear dipolar decoupling at ultra-fast MAS frequencies up to 65 kHz is shown in the present work. The advantage of lower RF amplitude requirement for RN_n^ν sequence over other methods at high MAS frequencies is discussed in the present work.

Acknowledgments

We thank National Facility for High Field NMR, TIFR. We thank Bruker Biospin GmbH for the use of 600 MHz spectrometer. We thank Shimon Vega and Malcolm Levitt for discussions.

References

[1] B.C. Gerstein, C. Clor, R.G. Pembelton, R.C. Wilson, Utility of pulse nuclear magnetic resonance in studying protons in coals, J. Phys. Chem. 81 (1977) 565.
[2] R.E. Taylor, R.G. Pembleton, L.M. Ryan, B.C. Gerstein, High resolution NMR in randomly oriented solids with homonuclear dipolar broadening: combined multiple pulse NMR and magic angle spinning, J. Chem. Phys. 71 (1979) 4541.
[3] B.C. Gerstein, CRAMPS: high resolution NMR of relatively high gamma nuclei, in: R.K. Harris (Ed.), Encyc. of Magn. Reson., John Wiley, 2009.
[4] E. Vinogradov, P.K. Madhu, S. Vega, High-resolution proton solid-state NMR spectroscopy by phase-modulated Lee-Goldburg experiment, Chem. Phys. Lett. 314 (1999) 443.
[5] E. Vinogradov, P.K. Madhu, S. Vega, A bimodal Floquet analysis of phase modulated Lee-Goldburg high resolution proton magic angle spinning NMR experiments, Chem. Phys. Lett. 329 (2000) 207.
[6] E. Vinogradov, P.K. Madhu, S. Vega, E. Vinogradov, P.K. Madhu, S. Vega, Phase modulated Lee-Goldburg magic angle spinning proton nuclear magnetic resonance experiments in the solid state: a bimodal Floquet theoretical treatment, J. Chem. Phys. 115 (2001) 8983.
[7] D. Sakellariou, A. Lesage, P. Hodgkinson, L. Emsley, Homonuclear dipolar decoupling in solid-state NMR using continuous phase modulation, Chem. Phys. Lett. 319 (2000) 253.
[8] P. Avenier, A. Lesage, M. Taoufik, A. Baudouin, A. De Mallmann, S. Fiddy, M. Vautier, L. Veyre, J.M. Basset, L. Emsley, E.A. Quadrelli, Well-defined surface imido amido tantalum(V) species from ammonia and silica-supported tantalum hydrides, J. Am. Chem. Soc. 129 (2007) 176.
[9] P.K. Madhu, X. Zhao, M.H. Levitt, High-resolution ^{1}H NMR in the solid state using symmetry-based pulse sequences, Chem. Phys. Lett. 346 (2001) 142.
[10] S. Paul, R.S. Thakur, P.K. Madhu, ^{1}H homonuclear dipolar decoupling at high magic-angle spinning frequencies with rotor-synchronised symmetry sequences, Chem. Phys. Lett. 456 (2008) 253.
[11] S. Paul, R.S. Thakur, M.H. Levitt, P.K. Madhu, Homonuclear dipolar decoupling using rotor-synchronised pulse sequences: towards pure absorption phase spectra, J. Magn. Reson. 205 (2010) 269.
[12] J.P. Amoureux, B.Hu.J. Trebosc, Enhanced resolution in proton solid-state NMR with very-fast MAS experiments, J. Magn. Reson. 193 (2008) 305.
[13] J.P. Amoureux, B.Hu.J. Trebosc, F. Deng, Homonuclear dipolar decoupling schemes for fast MAS, Solid State Nucl. Magn. Reson. 35 (2009) 19.
[14] M. Leskes, P.K. Madhu, S. Vega, Supercycled homonuclear dipolar decoupling in solid-state NMR: toward cleaner ^{1}H spectrum and higher spinning rates, J. Chem. Phys. 128 (2008) 052309.
[15] M. Leskes, S. Steuernagel, D. Schneider, P.K. Madhu, S. Vega, Homonuclear dipolar decoupling at magic-angle spinning frequencies up to 65 kHz in solid-state nuclear magnetic resonance, Chem. Phys. Lett. 466 (2008) 95.
[16] M. Leskes, P.K. Madhu, S. Vega, Why does PMLG proton decoupling work at 65 kHz MAS?, J Magn. Reson. 199 (2009) 208.
[17] E. Salager, R.S. Stein, S. Steuernagel, A. Lesage, B. Eléna, L. Emsley, Enhanced sensitivity in high-resolution ^{1}H solid-state NMR spectroscopy with DUMBO dipolar decoupling under ultra-fast MAS, Chem. Phys. Lett. 469 (2009) 336.
[18] E. Vinogradov, P.K. Madhu, S. Vega, Strategies for high-resolution proton spectroscopy in solid-state NMR, Top. Curr. Chem. 246 (2005) 33.
[19] D. Demco, S. Hafner, H.W. Spiess, Rotation-synchronized homonuclear dipolar decoupling, J. Magn. Reson. A 116 (1995) 36.
[20] S. Hafner, H.W. Spiess, Multiple-pulse line narrowing under fast magic-angle spinning, J. Magn. Reson. A 121 (1996) 160.
[21] S. Paul, P.K. Madhu, Homonuclear dipolar decoupling in solid-state nuclear magnetic resonance under the regime of moderate to high magic-angle spinning frequencies: a status report, J. IISc. 90 (2010) 1.
[22] C. Coelho, J. Rocha, P.K. Madhu, L. Mafra, Practical aspects of Lee-Goldburg based CRAMPS techniques for high-resolution ^{1}H NMR spectroscopy in solids, J. Magn. Reson. 194 (2008) 264.
[23] P.K. Madhu, High-resolution solid-state NMR spectroscopy of protons with homonuclear decoupling schemes under magic-angle spinning, Solid State Nucl. Magn. Reson. 35 (2009) 2.
[24] M.H. Levitt, Symmetry-based pulse sequences in magic-angle spinning solid-state NMR, in: D.M. Grant, R.K. Harris (Eds.), Encyc. of NMR, John Wiley & Sons, Chichester, 2002.
[25] S. Vega, Floquet theory, The Encyclopedia of Nuclear Magnetic Resonance, Wiley, London, 1995. p. 2011.
[26] M. Leskes, P.K. Madhu, S. Vega, Floquet theory in solid-state nuclear magnetic resonance, Prog. Nucl. Magn. Reson. Spectrosc. (2010), doi:10.1016/j.pnmrs.2010.06.002.
[27] G.J. Boender, S. Vega, H.J.M. De Groot, A physical interpretation of the Floquet description of magic angle spinning nuclear magnetic resonance spectroscopy, Mol. Phys. 95 (1998) 921.
[28] J.H. Van Vleck, On σ-type doubling and electron spin in the spectra of diatomic molecules, Phys. Rev. 33 (1929) 467.
[29] U. Haeberlen, High resolution NMR in solids – selective averaging, Adv. Magn. Reson. (Suppl. 1), Academic Press, New York, 1976.
[30] M. Leskes, P.K. Madhu, S. Vega, Proton line narrowing in solid-state nuclear magnetic resonance: new insights from windowed phase-modulated Lee-Goldburg sequence, J. Chem. Phys. 125 (2006) 124506 (1–18).
[31] K. Mao, M. Pruski, Homonuclear dipolar decoupling under fast MAS: resolution patterns and simple optimization strategy, J. Magn. Reson. 203 (2010) 144.